EUROPEAN ORGANIZATION FOR NUCLEAR RESEARCH

THE ENERGY DEPENDENCE OF THE PROTON-PROTON TOTAL CROSS-SECTION FOR CENTRE-OF-MASS ENERGIES BETWEEN 23 AND 53 GeV

U. Amaldi*), R. Biancastelli, C. Bosio and G. Matthiae,
Physics Laboratory, Istituto Superiore di Sanità
and INFN, Sezione Sanità, Rome, Italy.

J.V. Allaby, W. Bartel, G. Cocconi, A.N. Diddens, R.W. Dobinson
and A.M. Wetherell,
CERN, Geneva, Switzerland.

ABSTRACT

Measurements of proton-proton elastic scattering at angles around 6 mrad have been made at centre-of-mass energies of 23, 31, 45 and 53 GeV using the CERN Intersecting Storage Rings. The absolute scale of the cross-section was established by determination of the effective density of the colliding beams in their overlap region. Proton-proton total cross sections were deduced by extrapolation of the elastic differential cross-section to the forward direction and by application of the optical theorem. The results indicate that over the energy range studied the proton-proton total cross-section increases from about 39 to about 43 mb.

Geneva - January 1973

---

*) At present CERN Visiting Scientist.

The measurements of the strong interaction proton-proton total cross-section, σ_t, presently being performed at the CERN Intersecting Storage Rings (ISR) use methods other than the conventional transmission technique, which is not directly applicable to colliding beams. In one method σ_t is obtained from a measurement of the differential elastic scattering cross-section by application of the optical theorem[1,2], in another the total number of proton-proton interactions is counted[3]. In applying the first method two different approaches have been used to fix the absolute scale of the elastic cross-section: measurement of the elastic cross-section at very small momentum transfers[1], where Coulomb scattering is dominant and known in absolute value, and determination of the machine luminosity by the Van der Meer method[4,2].

This Letter presents measurements of σ_t at centre-of-mass energies, $\sqrt{s}$, of 23, 31, 45 and 53 GeV using the first method. The various steps involved may be summarized as follows:

a) Measurement of proton-proton elastic scattering at angles Θ around 6 mrad.

b) Determination of the effective density of the colliding beams in their overlap region (machine luminosity)by the Van der Meer method, which establishes the absolute scale of the differential cross-section $d\sigma/d\Omega$.

c) Extrapolation to $\Theta = 0$ using the measured Θ dependence of $d\sigma/d\Omega$.

d) Calculation of σ_t from the optical theorem.

The apparatus consisted of small scintillation counter hodoscopes measuring elastic scattering and of three monitor systems of large scintillators, detecting inelastic events at angles of about 50 mrad, to determine the ISR luminosity. At the beginning of each run the monitors were calibrated by means of the Van der Meer method[4], which may be described as follows.

The relationship between the counting rate R of a detector, registering events produced by two beams crossing in the horizontal plane, the cross-section $\Delta\sigma$ corresponding to the events counted by the detector and the vertical density distributions of the stored beam currents $i_1(z-z_1)$ and $i_2(z-z_2)$ may be written

$$R(\delta) = \frac{\Delta\sigma}{K} \int_{-\infty}^{+\infty} i_1(z)\, i_2(z+\delta)\, dz \,, \qquad (1)$$

where $\delta = z_1 - z_2$ is the vertical displacement between the centres z_1 and z_2 of the two beams. The constant K is given by

$$K = e^2\, \beta c\, \mathrm{tg}\left(\frac{\alpha}{2}\right) \,, \qquad (2)$$

α being the crossing angle of the beams at the ISR ($\alpha = 14.79^0 \pm 0.01^0$) and βc the velocity of the protons. Since the beams do not meet head-on, but each crosses the full horizontal width of the other, the collision probability does not depend on the shape of the density distribution in the horizontal direction, hence only the convolution of vertical density distributions is needed in Eq. (1). Following a suggestion of Van der Meer[4] a simple method has been used to determine the normalising factor $\Delta\sigma/K$ in Eq.(1). This method consists in measuring the counting rate $R(\delta)$ as a function of the vertical displacement δ between the two beams. The following relation then holds

$$\int_{-\infty}^{+\infty} R(\delta)\, d\delta = \frac{\Delta\sigma}{K}\, I_1\, I_2 \qquad (3)$$

because I_1 and I_2, the currents of the two circulating beams, are given by the expression $I = \int_{-\infty}^{+\infty} i(z)\, dz$.

In this experiment the integral $\int_{-\infty}^{+\infty} R(\delta)\, d\delta$ was measured by means of a monitor system which detected events from beam-beam collisions while the two beams were displaced vertically, one relative to the other, in small and precise steps (typically $\Delta\delta = 0.50 \pm 0.01$ mm at all energies). The experimentally determined integral, normalized to the product of the measured circulating currents (known to better than 10^{-4}) gives, using Eq.(3), the cross-section $\Delta\sigma_M$ for events which are within the acceptance of the monitor system. The procedure is valid only if the beam shapes are invariant during their displacements and only if the monitor rate is independent of the position of the source. To meet the second requirement a monitor which detects inelastic events is essential.

The relation between the "monitor constant" $\Delta\sigma_M$ and the elastic scattering cross-section $\Delta\sigma_E$ integrated over $\Delta\Omega$ is given by

$$\Delta\sigma_E = (d\sigma_E/d\Omega)\ \Delta\Omega = \Delta\sigma_M\ N_E/N_M\ , \qquad (4)$$

where N_E and N_M are the elastic and the monitor rates counted simultaneously. For Eq. (4) to be valid it is only necessary that the ISR energies are equal to those used for the calibration and that the monitor efficiency remains constant. The other parameters (such as beam currents, beam shapes etc.) can be changed at will and need not stay constant during the measurement of elastic scattering.

The counter arrangement used to measure elastic scattering events is shown schematically in Fig. 1. Protons scattered in the vertical plane were detected in coincidence by means of the two systems of scintillation counters A and B, each consisting of one hodoscope and two trigger counters, placed 9 m from the intersection region. Each hodoscope covered an area of 30 × 70 mm^2 and was formed by two separate arrays of horizontal and vertical scintillators. The horizontal scintillators H_i (i = 1, ...,5) were 6 mm high and 70 mm wide, while the vertical scintillators V_i (i = 1, ...,7) were 30 mm high and 10 mm wide. The effective size of each hodoscope element was thus determined by the height of the horizontal and the width of the vertical scintillators. The two arrays of horizontal and vertical scintillators were placed in between two trigger counters (called A', A'' and B', B'' for the A and B systems, respectively) of dimensions 35 × 75 mm^2, sufficient to cover the hodoscope scintillators.

A and B were placed in special, thin-wall sections (0.2 mm stainless steel) of the ISR vacuum chamber which could be displaced vertically towards the beams. The two hodoscopes were set symmetrically with respect to the crossing region to observe elastic scattering at angles around 6 mrad with the ISR operating at equal beam momenta.

The four-fold coincidence combination A'A''B'B'' was used to gate pattern units which registered the signals from the hodoscope

counters. The data, together with the time-of-flight between conjugate trigger counters and the pulse-heights of all counters, were recorded for each event. The rates of the three monitor systems were also recorded. A CAMAC system and a small on-line computer were used for data collection and storage on magnetic tape.

In order to have the crossing region small with respect to the size of the hodoscopes the data were taken with the machine working in the Terwilliger mode[5]. In this scheme, which uses special quadrupoles in the machine lattice, the width of the beams is determined only by the betatron oscillations. The distribution of the interaction points was approximately gaussian in shape with r.m.s. values of about 3 mm in the radial direction and about 1.5 mm in the vertical direction. Thus for the elastic (collinear) events, in which one of the scattered protons was detected close to the centre of one of the hodoscopes, the coincident proton was practically always detected by the other hodoscope. With stored currents of about 5 A the coincident rate at (22.6 + 22.6) GeV/c was about 20 events/sec; the accidental rate between hodoscopes A and B was always less than 1%.

In the data analysis only those triggers were used in which at least one array element of each hodoscope (out of twelve) had fired. This corresponded to the requirement of at least a six-fold coincidence. At all energies, about 72% of these triggers were events with one firing on a horizontal and a vertical counter in both hodoscopes. The events which fired two counters of the same array were about 16%. These events were interpreted as mostly due to δ-rays produced in the trigger counters or in the hodoscope scintillators. This interpretation agreed with measurements performed in a particle beam in connection with a previous experiment[1]. Six per cent of the triggers were multiple firings, which were attributed either to interactions in the vacuum chamber of elastically scattered protons or to true inelastic processes coming from the source. In about 6% of the events one of the four arrays gave no signal. The number of these blank events agreed with estimates based on the measured spacing between adjacent counters of the arrays.

The events (with the exclusion of blank events) were displayed in matrices according to the following procedure. Consider the centre element of hodoscope A as the element defining the solid angle $\Delta\Omega$, i.e. the element $(H_3V_4)_A$. Elastic events registering in this element have their conjugate proton distributed over hodoscope B. The events in which only this element of hodoscope A was fired and, on the opposite hodoscope B, there was only one firing of a horizontal counter H_i and one firing of a vertical counter V_j, were added with weight 1 to the matrix element ij. For multiple events (both of A and/or B hodoscopes) weights smaller than 1 were attributed to each possible AB combination in such a way that each detected event was counted only once. In this manner the total number of elastic events in the sample was not altered, independent of whether a δ-ray was produced or the scattered proton had interacted in the chamber wall or in the counters. An example of a $(H_iV_j)_B$ matrix obtained in a run at (26.6 + 26.6), GeV/c selecting the central element $(H_3V_4)_A$ of the A hodoscope, is shown in Fig. 2. The total number of events in this matrix is about 5500. The kinematic correlation typical of elastic scattering events produced a prominent peak over a small background, caused by inelastic processes. The dimensions of the source and of the counters fixed the definition of elastic events, which corresponded to the criterion that two charged particles were collinear with an r.m.s. angle of ± 1 mrad in the horizontal and ± 0.4 mrad in the vertical plane. These angles correspond to transverse momenta of about 20 MeV/c, small enough to ensure that the contribution of any other known physical process has a much wider distribution. In particular, since the typical transverse momenta in the decay of a diffractively produced resonance are about 200 MeV/c, the distribution of the decay particles is practically uniform below the peak of Fig. 2 and contributes to the uniform background, which is subtracted. Unknown phenomena of sizeable cross-sections, having characteristic transverse momenta smaller than $\sim$ 20 MeV/c, would invalidate the present definition of elastic events.

The procedure described above for the central element $(H_3V_4)_A$ of hodoscope A has been applied to the nine central elements of hodoscopes A and B. The elastic event rate N_E introduced in Eq. (4) was then

obtained by subtracting a common background from the matrices corresponding to these nine central elements $H_i V_j$ (i = 2,3,4 and j = 3,4,5) of the hodoscopes. The percentage values of the background, subtracted at the four different ISR momenta of (11.8 + 11.8), (15.4 + 15.4), (22.6 + 22.6) and (26.6 + 26.6) GeV/c were 3.5%, 5.0%, 7.5% and 10%, respectively, and were obtained by means of a computer program which fitted the shape of the peak in the matrix. For the nine combinations chosen the elastic peak was quite well centred on the matrix itself so that the border losses due to the finite extension of the hodoscope arrays were small (less than 2%) and could be safely estimated.

In applying Eq. (4) the main source of error turned out to be the uncertainty in the monitor constant $\Delta\sigma_M$ so that three independent monitor systems, M_1, M_2 and M_3, were used. Each monitor consisted of two pairs of scintillation counters placed about 5 m from the intersection region to detect mainly inelastic beam-beam collisions. The dimensions of these counters were 20 × 30 cm^2 for monitor M_1, 40 × 40 cm^2 for M_2, and 50 × 50 cm^2 for M_3. In order to avoid orbit distortions induced by simultaneous displacements of the beams in the other intersection regions, many special calibration runs were performed, at the four ISR energies, by displacing vertically the beams only in the intersection region where the apparatus was mounted. The absence of beam blow-up effects for high intensities (i.e. beam currents >5 A) was established by calibration runs at (26.6 + 26.6) GeV/c in which the product of currents ($I_1 \times I_2$) was varied by a factor of ten and in which the vertical heights of the beams was changed by a factor of two. The observed maximum spread of the most stable monitor at any given energy in any condition was ±2% over a period of about two months. The cross-sections were computed using this monitor and attributing to the determination of the monitor constant $\Delta\sigma_M$ a standard deviation of 2%, equal to the observed maximum spread.

Having obtained the elastic differential cross-section at angles around 6 mrad the Coulomb contribution, which varied from ∿ 5% at (11.8 + 11.8) GeV/c to ∿ 0.2% at (26.6 + 26.6) GeV/c, was subtracted and

the extrapolation of the nuclear scattering differential cross-section $d\sigma/dt = (\pi/p^2)\, d\sigma/d\Omega$ to the forward direction was performed using the expression

$$(d\sigma/dt) = (d\sigma/dt)_{t=0}\, e^{bt} \quad . \tag{5}$$

The forward scattering cross-section was then related to the total cross-section σ_t through the optical theorem:

$$\sigma_t = \sqrt{\frac{16\pi}{(1+\rho^2)} \left(\frac{d\sigma}{dt}\right)_{t=0}} \quad . \tag{6}$$

The previous equations are based on the assumptions that the nuclear differential cross-section depends exponentially on the square of the four-momentum transfer, t, with a constant slope parameter b down to zero scattering angles, and that spin effects are negligible. The validity of these assumptions was discussed in Ref. 1. The ratio of the real to the imaginary part of the nuclear amplitude, ρ, has been previously measured[1] and its average value between $\sqrt{s}$ = 23 and 31 GeV was found to be $\rho = 0.025 \pm 0.035$. Since the result is compatible with $\rho = 0$, this value has been assumed in applying Eq. (6). The presence of a small real part does not affect the determination of σ_t. In fact an uncertainty of $\Delta\rho = \pm 0.05$ would cause a decrease of σ_t of only 0.05 mb.

Table 1 gives the momentum transfers $|t|$ at which the elastic scattering was measured, the values of the differential cross-section $d\sigma/dt$, the parameters b used, the extrapolation factors $e^{b|t|}$ and the forward nuclear cross-section $(d\sigma/dt)_{t=0}$.

The values of b used in Eq. (5) and shown in Table 1 were obtained by interpolation of previous measurements[6,7] taken together with new values obtained at $\sqrt{s}$ = 45 and 53 GeV with the apparatus described in a previous publication[1]. The new results are: $b = (12.6 \pm 0.4)$ GeV^{-2} in the range $0.01 \leq |t| \leq 0.05$ GeV at $\sqrt{s}$ = 45 GeV and $b = 13.1 \pm 0.3$ GeV^{-2} in the range $0.01 \leq |t| \leq 0.06$ GeV^2 at 53 GeV. These values agree well with the figures obtained at somewhat larger momentum

transfers[6], which supports the assumption that for $|t| \lesssim 0.1$ GeV the value of b in Eq. (5) remains constant.

The sources of the errors on the extrapolated differential cross-sections are listed in Table 2. As discussed previously, the biggest contribution arises from the uncertainty in the measurement of the monitor constant. A safe estimate has been made for the error introduced by the inelastic background subtraction, since the error has been taken equal to 15% of the background itself. In addition, the effect of a generous error $\Delta b = \pm 0.5$ GeV^{-2}, which is about twice the experimental error, has been taken into account in Table 2.

The errors appearing in Tables 1 and 2 are point-to-point errors. In addition there is a scale error which affects equally the measured differential cross sections at the four momenta, with an estimated standard deviation of 3%. It was obtained by combining estimated errors of ±2% due to calibration of the magnets which displace vertically the beams in the ISR, ±2% due to uncertainty in the knowledge of the solid angle $\Delta\Omega$, ±0.5% due to possible counter inefficiencies, and ±1% due to the uncertainty in the background subtraction of the blank events and in the estimate of the border losses.

Table 3 contains the total cross-section obtained from Eq.(6). Note that percentage-wise the errors in σ_t are one-half of the errors in $(d\sigma/dt)_{t=0}$ because this enters under the square root in Eq.(6). The fifth column of the table gives the total elastic cross-sections σ_{el} computed using the extrapolated values of the forward cross-section with the quoted slopes for $|t| \leq 0.1$ GeV^2, and an exponential behaviour of smaller slope for $|t| \gtrsim 0.1$ GeV^2 as measured by Barbiellini et al[7]. In the last column the total inelastic cross section $\sigma_{in} = \sigma_t - \sigma_{el}$ is given.

The values of the total cross-sections are plotted in Fig. 3 together with other published data[1,8] as well as the antiproton-proton cross-section up to 50 GeV/c. The present results at $\sqrt{s}$ = 23 and 51 GeV, (σ_t = (39.1 ± 0.7)mb and σ_t = (40.5± 0.8) mb, respectively) can be compared with the values obtained at the same energies by using Coulomb scattering to normalize the cross-section scale[1]: (38.9 ± 0.7) mb and (40.2 ± 0.8) mb, respectively. The average difference is (0.25 ± 0.75) mb, well within the

errors. This good agreement demonstrates that at these two energies the evaluations of the luminosity by the Van der Meer and the Coulomb scattering methods agree within (1 ± 4)%.

The main conclusion of this experiment is that the proton-proton total cross-section increases by

$$\Delta\sigma_t = (4.1 \pm 0.7) \text{ mb} \qquad (7)$$

when the centre-of-mass energy increases from 23 to 53 GeV. The present ISR data alone may be fitted by a linear increase with ℓn s. On the other hand, Fig. 3 indicates that σ_t goes through a shallow minimum around $s_0 = 200$ GeV^2 where $\sigma_t = \sigma_0 = (38.4 \pm 0.3)$ mb. Thus, over a wider energy range, $100 \lesssim s \lesssim 2800$ GeV^2 an expression of the form

$$\sigma = \sigma_0 + \sigma_1 \left[\ell n\ (s/s_0)\right]^{\nu} \qquad (8)$$

provides a good fit to the data with $\sigma_1 = (0.9 \pm 0.3)$ mb and $\nu = 1.8 \pm 0.4$. Such an increase of the total nuclear cross-section with energy agrees, within a large error and over this energy range, with the Froissart limit, $\nu = 2$, which corresponds to the maximum rate of increase allowed by unitarity[9].

Cosmic-ray data have recently been interpreted as suggesting a similar behaviour[10] for σ_{in}. An increase of σ_{in} proportional to $(\ell n\ s)^2$ was first suggested by Heisenberg[11] as a consequence of his bremsstrahlung model of multiple production.

The present results, together with previous data, lead to the following picture of proton-proton interactions at the highest energies attainable with present accelerators.

i) The slope b of the forward elastic differential cross section increases monotonically with energy[6,7]. In the ISR energy range explored the increase is (11 ± 3)%.

ii) The ratio ρ of the real to the imaginary parts of the forward scattering amplitude increases from about -0.1 at $\sqrt{s} = 10$ GeV [12] to a value consistent with zero, $\rho = 0.025 \pm 0.035$ at $\sqrt{s} = 25$ GeV [1].

iii) The total nuclear cross-section goes through a shallow minimum at $\sqrt{s} \simeq 15$ GeV and then increases by nearly 5 mb as the energy increases to $\sqrt{s} = 53$ GeV. In the ISR energy range the increase is $(10 \pm 2)\%$.

iv) The elastic cross-section σ_{el} starts to increase from a similar shallow minimum at a similar value of the centre-of-mass energy. In the ISR range the increase is $(12 \pm 4)\%$. This is understandable from points (i) and (iii) above, since integration of Eq. (5) gives $\sigma_{el} \propto \sigma_t^2/b$. (The change of slope beyond $|t| \simeq 0.1$ GeV^2 gives a correction of a few per cent to this expression.)

v) The inelastic cross-section, $\sigma_{in} = \sigma_t - \sigma_{el}$, thus also increases by about $(10 \pm 2)\%$ in the ISR range.

The approximate equality of the relative increases of b, σ_t, σ_{el} and σ_{in} in the ISR energy range is consistent with a naïve optical model of an absorbing disc of constant opacity, since in such a picture all four quantities are proportional to R^2, where R is the interaction radius of the scattering particles. Within this framework the data indicate that the radius R increases by about 5% when the centre-of-mass energy increases from $\sqrt{s} = 23$ to 53 GeV.

The following final remarks may be made. It has been found by Denisov et al.[8] that the K^+- p cross-section increases, from a constant plateau of 17 mb below 20 GeV/c, to about 18 mb at 55 GeV/c. Considering the trend of the antiproton-proton cross-section shown in Fig. 3 it is conceivable that this cross-section passes through a minimum at a value of $s \gtrsim 300$ GeV^2 before rising towards the p-p cross section, if there is a common high-energy limit as required by the Pomeranchuk theorem. One may then speculate that the K^+- p, p-p and $\bar{p}$-p total cross-sections begin to increase at energies connected with the magnitude of their plateau cross-sections, the rise appearing at lower energy the smaller the cross-section of the plateau. One would thus expect that the total cross-sections for K^-- p, π^+- p and π^-- p will also rise appreciably at laboratory momenta above 60 GeV/c, but in all three cases at momenta lower than that at which the p-p cross section begins to rise.

We are indebted to the staff of the various sections of the ISR Department for having provided the precise and stable beams vital to this experiment. In particular we are grateful to P. Bryant and K.M. Potter for their work in improving the precision of the luminosity measurements, and to J.-C. Brunet, J.-C. Godot, E. Jones and G. Rollinger for their essential contribution in the construction of the special vacuum chamber. We are very grateful for the help in data analysis given by Mme C. Busi. The excellent technical support of R. Donnet, M. Ferrat and C.A. Ståhlbrandt of CERN and of P. Gricia, R. Orlando and P. Veneroni of Rome is acknowledged. We also thank the Aachen-CERN-Genova-Harvard-Torino group for the use of one of their monitors and for useful discussions. Z. Dimcovski is thanked for valuable contributions to the experiment.

Table 1

Measured elastic differential cross section

ISR Momentum (GeV/c)	$\|t\|$ (GeV^2)	$(d\sigma/dt)$ (mb/GeV^2)	b (GeV^{-2})	$e^{b\|t\|}$ extrapolation factor	$(d\sigma/dt)_{t=0}$ (mb/GeV^2)
(11.8+11.8)	$8.1\ 10^{-3}$	71.0±1.5	11.8	1.10	78.1±1.7
(15.4+15.4)	$13.5\ 10^{-3}$	71.0±1.6	12.3	1.18	83.8±1.9
(22.6+22.6)	$17.5\ 10^{-3}$	73.8±1.7	12.8	1.25	92.3±2.2
(26.6+26.6)	$23.0\ 10^{-3}$	70.6±1.8	13.1	1.35	95.4±2.6

Table 2

Point-to-point errors

Source of error	Percentage standard deviation on $(d\sigma/dt)_{t=0}$			
	11.8 GeV/c	15.4 GeV/c	22.6 GeV/c	26.6 GeV/c
Monitor constant $\Delta\sigma_M$	± 2.0%	±2.0%	±2.0%	±2.0%
Statistics	< 0.5%	<0.5%	<0.5%	<0.5%
Subtraction of inelastic background	± 0.5%	±0.7%	±1.0%	±1.5%
Coulomb subtraction	± 0.3%	±0.1%	-	-
Error in the slope parameter ($\Delta b = \pm 0.5\ GeV^{-2}$)	± 0.4%	±0.6%	±0.7%	±1.0%
Overall error	± 2.2%	±2.3%	±2.4%	±2.7%

Table 3

Total and elastic cross sections

ISR momenta GeV/c	c.m. energy $\sqrt{s}$ (GeV)	Equivalent laboratory momentum (GeV/c)	σ_t (scale error= ±0.6 mb)*) (mb)	σ_{el} (scale error= ±0.3 mb) (mb)	σ_{in} (scale error= ±0.5 mb) (mb)
(11.8+11.8)	23.5	290	39.1±0.4	6.8±0.2	32.3±0.4
(15.4+15.4)	30.6	500	40.5±0.5	7.0±0.2	33.5±0.4
(22.6+22.6)	44.9	1070	42.5±0.5	7.5±0.3	35.0±0.5
(26.6+26.6)	52.8	1480	43.2±0.6	7.6±0.3	35.6±0.5

*) When comparing with results of other experiments the point-to-point errors should be combined quadratically with the scale errors.

REFERENCES

1. U. Amaldi, R. Biancastelli, C. Bosio , G. Matthiae, J.V. Allaby, W. Bartel, M.M. Block, G. Cocconi, A.N. Diddens, R.W. Dobinson, J. Litt and A.M. Wetherell, Phys.Letters (in print).

2. M. Holder, E. Radermacher, A. Staude, G. Barbiellini, P. Darriulat, M. Hansroul, S. Orito, P. Palazzi, A. Santroni, P. Strolin, K. Tittel, J. Pilcher, C. Rubbia, G. De Zorzi, M. Macri, G. Sette, C. Grosso-Pilcher, A. Fainberg and G. Maderni, Phys.Letters 35B (1971) 361.

3. An experiment along these lines is presently being performed at the ISR by the Pisa-Stony Brook collaboration.

4. S. Van der Meer, CERN Internal Report ISR-PO/68-31 (1968), unpublished.

5. K.M. Terwilliger, Proceedings of the International Conference on High Energy Accelerators (CERN), p. 53 (1959).

6. U. Amaldi, R. Biancastelli, C. Bosio, G. Matthiae, J.V. Allaby, W. Bartel, G. Cocconi, A.N. Diddens, R.W. Dobinson, V. Elings, J. Litt, L.S. Rochester and A.M. Wetherell, Phys.Letters 36B (1971) 504.

7. M. Holder, E. Radermacher, A. Staude, G. Barbiellini, P. Darriulat, M. Hansroul, S. Orito, P. Palazzi, A. Santroni, P. Strolin, K. Tittel, J. Pilcher, C. Rubbia, G. De Zorzi, M. Macri, G. Sette,C.Grosso-Pilcher, A. Fainberg and G. Maderni, Phys.Letters 35B (1971) 355.

   M. Holder, E. Radermacher, A. Staude, G. Barbiellini, P. Darriulat, P. Palazzi, A. Santroni, P. Strolin, K. Tittel, J. Pilcher, C. Rubbia, M. Bozzo, G. De Zorzi, M. Macri, S. Orito, G. Sette, A. Fainberg, C. Grosso-Pilcher and G. Maderni, Phys.Letters 36B (1971) 400.

   G. Barbiellini, M. Bozzo, P. Darriulat, G. Diambrini-Palazzi, G. De Zorzi, A. Fainberg, M.I. Ferrero, M. Holder, A. McFarland, G. Maderni, S. Orito, J. Pilcher, C. Rubbia, A. Santroni, G. Sette, A. Staude, P. Strolin and K. Tittel, Phys.Letters 39B (1972) 663.

8. S.P. Denisov, S.V. Donskov, Yu.P. Gorin, A.I. Petrukhin, Yu.D.Prokoshkin, D.A. Stoyanova, J.V. Allaby and G. Giacomelli, Phys.Letters 36B (1971) 415.

   J.W. Chapman, N. Green, B.P. Roe, A.A. Seidl, D. Sinclair, J.C. Van der Velde, C.M. Bromberg, D. Cohen, T. Ferbel, P. Slattery, S. Stone and B. Werner, Phys.Rev.Letters 29 (1972) 1686.

REFERENCES (cont'd)

8. G. Charlton, Y. Cho, M. Derrick, R. Engelmann. T. Fields, L. Hyman, K. Jaeger, U. Mehtani, B. Musgrave, Y. Oren, D. Rhines. P. Schreiner, H. Yuta, L. Voyvodic, R. Walker, J. Whitmore, H.B.Crawley, Z. Ming Ma and R.G. Glasser, Phys.Rev.Letters 29 (1972) 515.

   F.T. Dao, D. Gordon, J. Lach, E. Malamud, T. Meyer, R. Poster and W. Slater, Phys.Rev.Letters 29 (1972) 1627.

9. M. Froissart, Phys.Rev. 123 (1961) 1053.

   A. Martin, Phys.Rev. 129 (1963) 1432 and Nuovo Cimento 42 (1966) 930.

10. G.B. Yodh, Yash Pal and J.S. Trefil, Phys.Rev.Letters 28 (1972) 1005.

11. W. Heisenberg, in Kosmische Strahlung (Springer Verlag 1953) p. 148.

12. G.C. Beznogikh, A. Bujak, L.F. Kirillova, B.A. Morozov, V.A. Nikitin, P.V. Nomokonov, A. Sandacz, M.G. Shafranova, V.A. Sviridov, Truong Bien, V.I. Zayachki, N.K. Zhidkov and L.S. Zolin, Phys.Letters 39B (1972), 411, and Dubna preprint E1-6613 (1972), to be published in Nucl.Physics.

Figure captions

Fig. 1 : General layout of the experimental apparatus and sketch of the disposition of hodoscopes in the special vacuum chamber sections.

Fig. 2 : Three-dimensional representation of the coincidence rate between the central element of hodoscope A and the 35 elements of hodoscope B obtained in a run of about one hour at (26.6 + 26.6) GeV/c.

Fig. 3 : Total proton-proton cross-sections as a function of the square of the centre-of-mass energy, s, and of the equivalent laboratory momentum. The general trends of the proton-proton data below 15 GeV/c and of the antiproton-proton cross-sections are indicated by smooth curves. The previous high-energy data are taken from references 1, 2 and 8. When comparing the results of the present experiment with lower energy data, a systematic error of ±0.6 mb should be combined with the point-to-point errors shown in the figure.

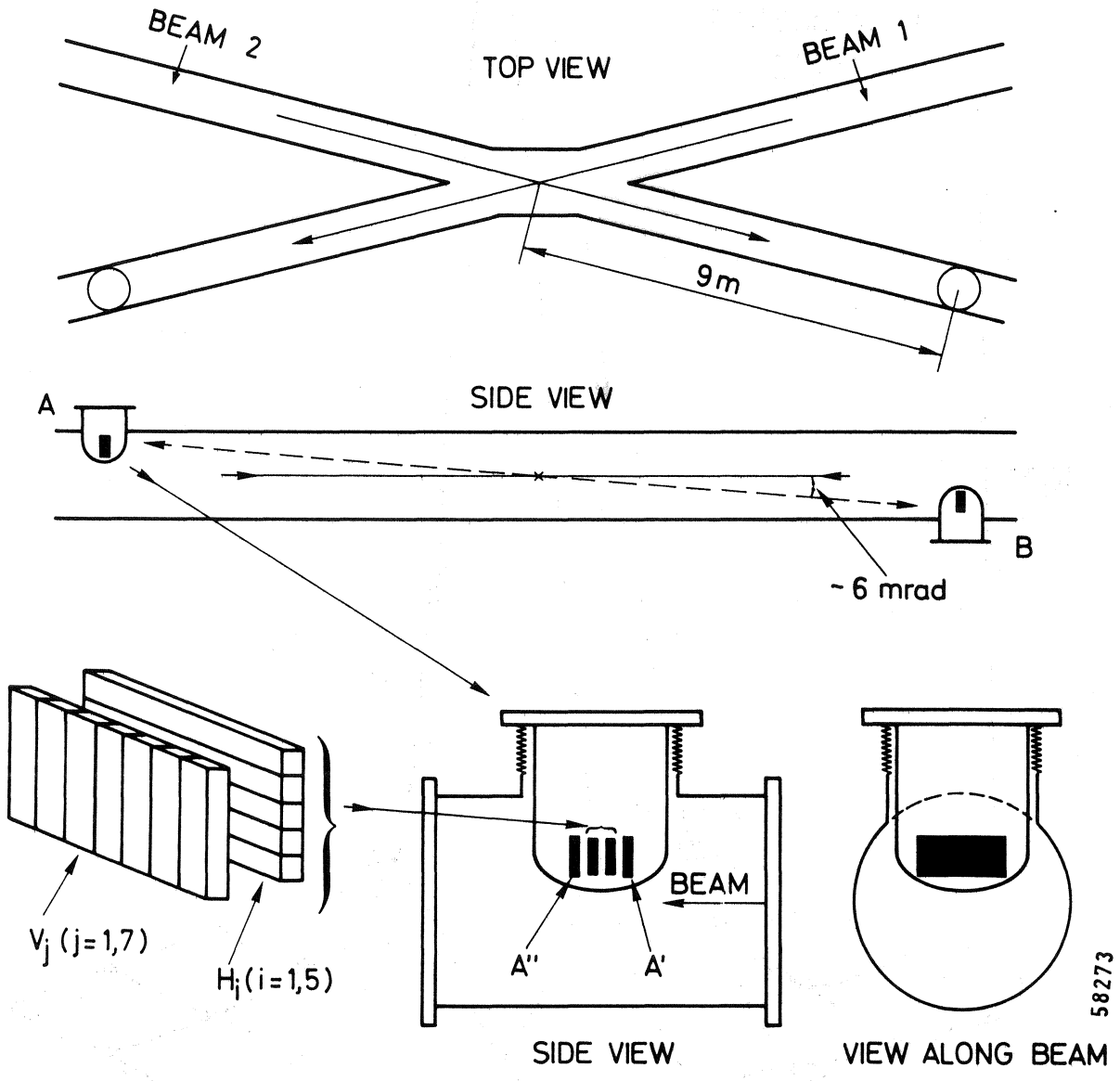
BEAM 2
TOP VIEW
BEAM 1
9m
A
SIDE VIEW
B
~ 6 mrad
V_j (j=1,7)
H_i (i=1,5)
BEAM
A''
A'
SIDE VIEW
VIEW ALONG BEAM
58273

FIG.1

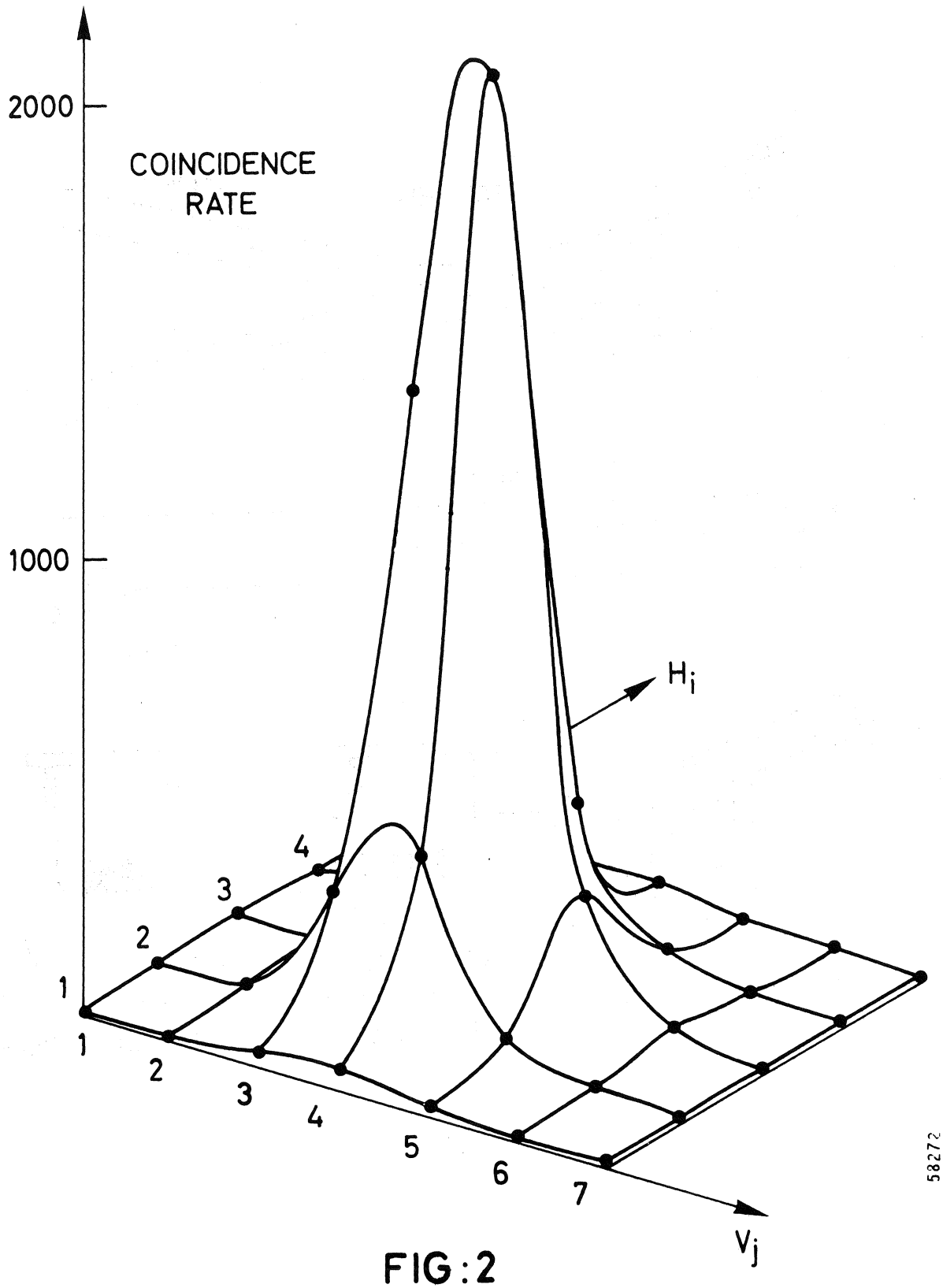

FIG:2

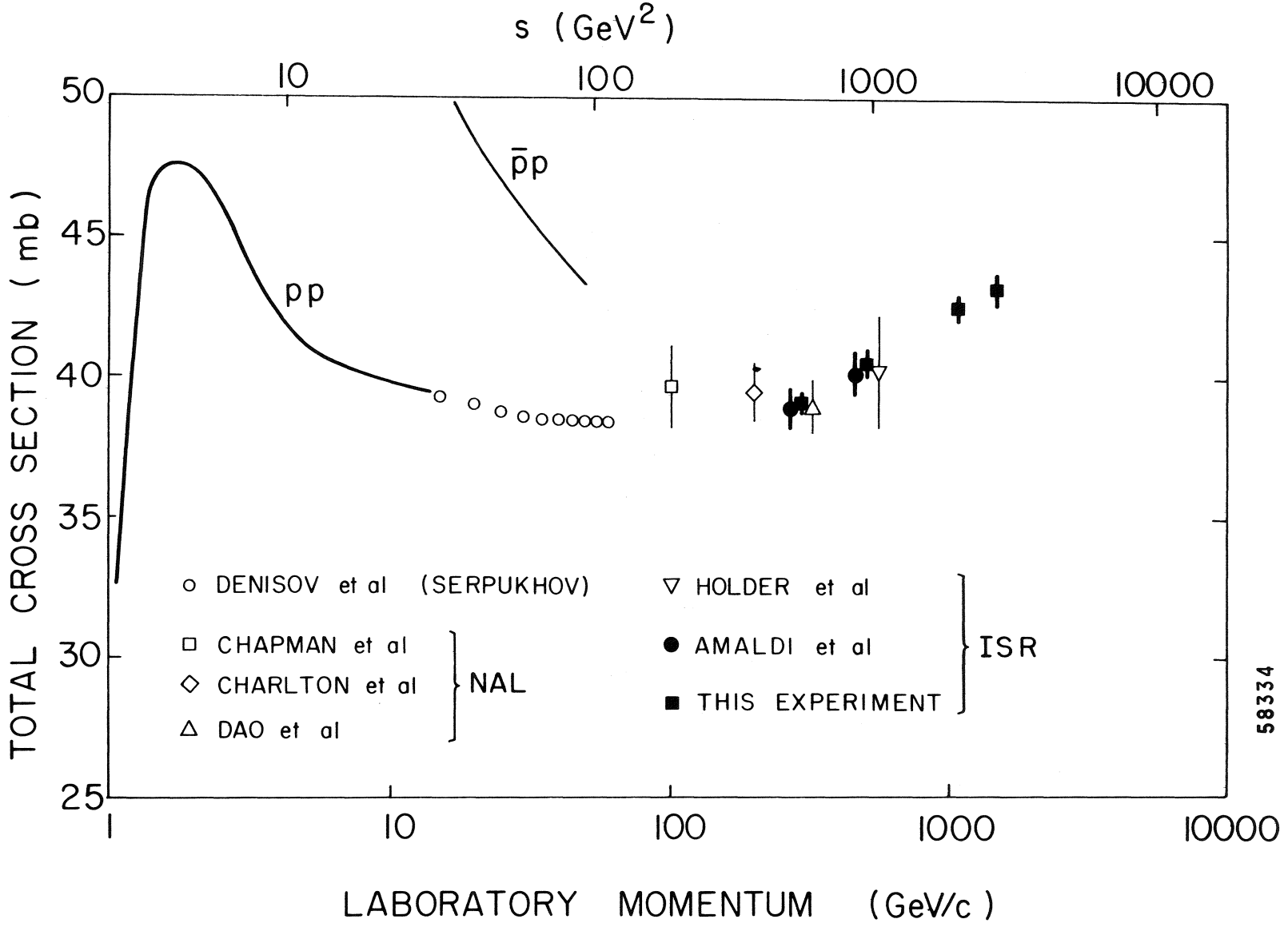
s (GeV²)
10
100
1000
10000
50
45
40
35
30
25
TOTAL CROSS SECTION (mb)
p̄p
pp
DENISOV et al (SERPUKHOV)
CHAPMAN et al
CHARLTON et al
DAO et al
NAL
HOLDER et al
AMALDI et al
THIS EXPERIMENT
ISR
58334
1
10
100
1000
10000
LABORATORY MOMENTUM (GeV/c)

FIG:3